X-ray Jets

Aneta Siemiginowska

The first recorded observation of an extragalactic jet was made almost a century ago. In 1918 Heber Curtis, an astronomer in the Lick Observatory, published "Descriptions of 762 nebulae and clusters photographed with the Crossley Reflector." He wrote a note by the entry for NGC 4486 (M87): "*A curious straight ray lies in a gap in the nebulosity in p.a. 20 deg apparently connected with the nucleus by a thin line of matter. The ray is brightest at its inner end, which is 11 arcsec from the nucleus*."

A few decades later Baade & Minkowski (1954) published an optical image of M87 showing 20 arcsec long and 2 arcsec wide jet with clear condensations along the jet. It is surprising to read their statement: "*No possibility exists at this time of forming any hypothesis on the formation of the jet, the physical state of its material, and the mechanism which connects the existence of the jet with the observed radio emission*."

This was 1954, the era of pre-digital astronomy, when image analysis was based on photographic plates and performed by eye, with a ruler and a pencil. Only a few radio sources had been identified at that time, quasars had yet to be discovered, and a few more decades had to lapse before the first X-ray observations of jets. The Einstein High Resolution Imager (HRI) provided the first X-ray data of M87 jet (Feigelson 1980; Schreier et al. 1982). The first jet discovered in X-rays was the jet of a radio galaxy Centaurus A which was later studied in radio wavelengths (Schreier et al. 1979). The Einstein HRI image of the famous quasar 3C273 needed careful analyses to discern X-rays emitted by the relativistic jet (Willingale 1981). Later on ROSAT provided a few more detections of jets, but only with *Chandra* did X-ray studies of large scale jets become routine.

During the past 15 years the *Chandra* X-ray Observatory has performed many observations of jets in a variety of objects, from stellar types in our galaxy to quasars in the high redshift universe. Understanding jets might bring us closer to understanding the physics of accreting systems across many different scales. While the observational data gathered over these past years underlined the significance of jets in the evolution of galaxies and clusters of galaxies, there are still many unanswered questions, including the nature of relativistic jets, jet energetics, particle content, particle acceleration and emission processes. Both statistical studies of large samples of jets across the entire electromagnetic spectrum and deep broad-band images of individual jets are necessary to tackle some of these questions.

In the *Chandra* Newsletter #13 (2006) Schwartz and Harris introduced the studies of X-ray jets which became possible with the high angular resolution X-ray mirrors provided by *Chandra*. Most of the X-ray jets remain unresolved in *XMM-Newton* or *Suzaku* observations and *Chandra* is critical to all the high angular resolution observations revealing the X-ray structures on sub-arcsec scales. In this letter I highlight some recent results of extragalactic jet studies with *Chandra* and direct the readers to more detailed reviews of the field given by Harris & Krawczynski (2006), Worrall (2009), and Pudritz et al. (2012).

Chandra Observations

The many discoveries of X-ray jets thrilled scientists in the early days of *Chandra*. They included the discovery of the PKS 0637-752 (Tavecchio et al. 2000, Cellotti et al. 2001, Schwartz et al. 2000) jet in the first calibration observation designed to test the focus of the mirrors on orbit. The initial discoveries were followed by a few systematic surveys to find X-ray jets and also by detailed studies of a few jets. The X-ray jets are seen as diffuse linear and bending structures with enhancements due to knots or hot spots. The jet is often located close to the strong core emission, or embedded in the diffuse emission of a host galaxy with a total length rarely exceeding $\sim 30''$. Most X-ray jets are rather faint and their emission is only a small (< 3%) fraction of a strong core, the main reason why only a few jets were detected in earlier X-ray missions. *Chandra* opened a new window to the studies of relativistic extragalactic jets.

Several surveys of X-ray jets have been completed to date. They differ in their selection criteria, but all originated from samples of known radio jets. Sambruna et al. (2004) selected 17 radio jets from a list of known AGN jets. These radio jets were longer than $3''$ and bright ($S_{1.4GHz} > 5$mJy arcsec^{-2}), with at least one knot located at a large distance from the nucleus. The sample of Marshall et al. (2011) contained 56 flat spectrum radio quasars compiled from VLA and ATCA

imaging radio surveys and selected targets based on the flux density in the extended emission and the radio jet morphology. This sample was divided into two sub-classes: A – purely jet flux limited and B – based on radio morphology and biased toward one-sided and linear structure. In both surveys the *Chandra* observations were short (< 10 ksec), but about 60% of these radio jets were detected in X-rays. A higher fraction of resolved X-ray jets, 78%, in similar *Chandra* exposures was found by Hogan et al. (2011) in a sample of 13 blazars selected from the flux-limited MOJAVE sample of relativistic jets associated with quasars and FR II radio galaxies.

Most of the survey studies focused on understanding the X-ray emission process in large scale extragalactic jets. The possible mechanisms include synchrotron emission from highly relativistic particles in the jet or the emission resulting from the inverse Compton process where such particles transfer energy to lower frequency photons (radio-IR-optical-UV) resulting in the X-ray emission. The source of the photon field could be internal to the jet (synchrotron-self-Compton, SSC) or external to the jet. In the large scale jets associated with quasars, the Cosmic Microwave Background was considered as the likely primary source of the photon field (IC/CMB).

Current observations indicate that synchrotron emission is the primary process producing X- rays in jets associated with low power radio galaxies classified as FRI. M87 and Centaurus A are examples of nearby FRI galaxies where the jets were studied in great detail. Both jets exhibit a correlated morphology (see M87 Fig. 1). The simple "one-zone" model where the radio and X-ray emission are produced by the same population of relativistic particles is supported by the observations. However, some evolution of the electron energy spectrum along the jet is required for these two cases. Recent studies of the archival *Chandra* data of FRI jets by Harwood & Hardcastle (2012) indicate no statistically significant correlations between the properties of the host galaxy and the jet, but show that the luminosity of X-ray jets scales linearly with the jet radio luminosity and that the X-ray spectral slope is related to both X-ray and radio luminosity of the jet. Since the X-ray emission in these jets is due to synchrotron processes, the particle acceleration mechanisms could be tested, but the sample of the suitable FRI jets is still limited.

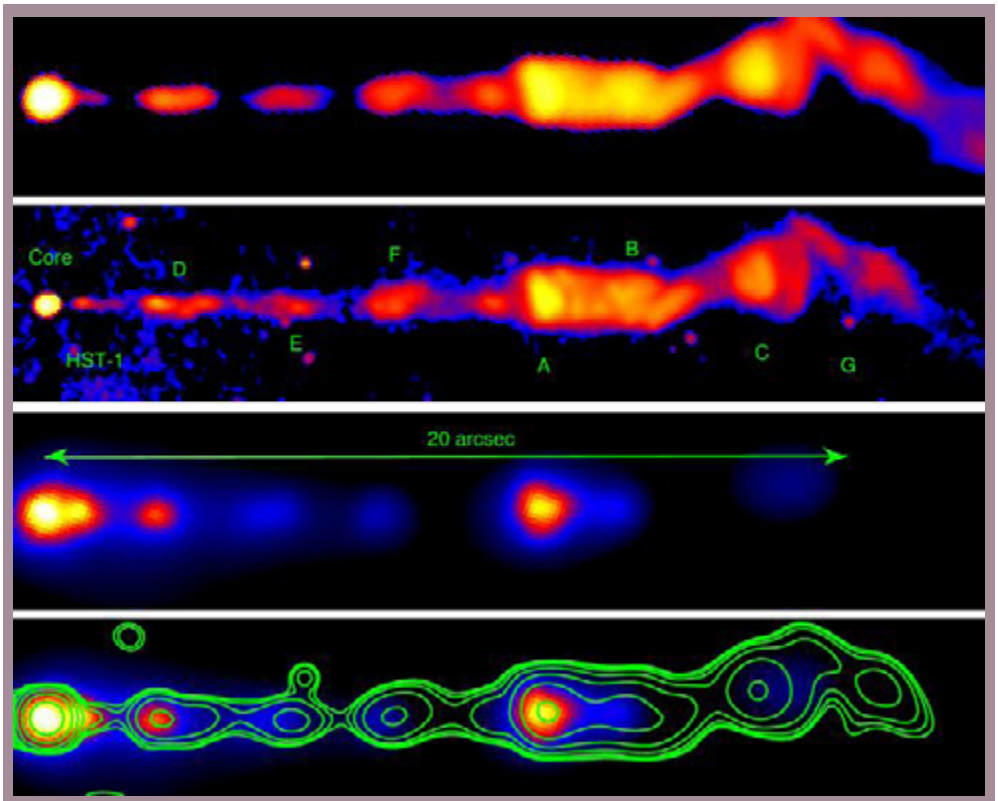

Fig. 1 — M87 jet in three bands, rotated to be horizontal (from Marshall et al. (2002)). Top: VLA image at 14.435 GHz with spatial resolution ~ 0.2". Second panel: The HST Planetary Camera image in the F814W filter from Perlman et al. (2001). Third panel: Adaptively smoothed Chandra *X-ray image. Lower panel: Smoothed* Chandra *image overlaid with contours of a Gaussian smoothed HST image matching the* Chandra *PSF. The HST and VLA images have a logarithmic stretch to bring out faint features, while the X-ray image scaling is linear.*

Harris, Massaro and Cheung compiled a list of all X-ray jets detected with *Chandra* and made the radio and X-ray data available on the web page: http://hea-www.harvard.edu/XJET/. They (Massaro et al. 2011) used these data to describe statistical properties of all the detected X-ray jet features, knots, hot spots, diffuse jet emission. The archival sample is heterogeneous, consists of 106 sources (FRI and FRII radio galaxies and quasars) and shows

a total of 236 detected jet related features. The redshift coverage at $z < 1$ is relatively good, but there are only a few sources at $z > 2$. This sample represents a variety of radio sources with X-ray jets in the *Chandra* archives to date. The statistical studies are still limited to small numbers and basic questions about the X-ray emission process or particle acceleration remain unanswered. However, there are interesting results indicating a real difference in the radio to X-ray flux ratios between the hotspots and knots in FRII sources (see 3C353 in Fig. 8), and no significant difference in the ratios for the knots in FRI and quasar jets. This second result suggests that either the knots in both types of jets are due to the synchrotron process, or that the inverse Compton process in quasar knots has very specific conditions resulting in the same flux ratios. A large sample of quasar jets, especially at high-z is needed to address these issues.

Quasar Jet Power

The total jet power, i.e. integrated over the entire lifetime of the jet, has been measured via X-ray cavities in X-ray clusters. This power can suppress cluster cooling and is therefore critical to the evolution of such structures in the universe. However, the instantaneous jet power carries the details of the jet launching physics yet is much harder to assess. The history of jet formation is imprinted into the jet X-ray emission, but is difficult to read unless we understand the primary emission processes in the jet. If the X-ray emission of quasar jets is predominantly due to inverse Compton scattering of the CMB, then under certain assumptions the bulk motion of the jet could be measured. High quality *Chandra* data with additional multiband radio and optical data are necessary to constrain the models (see, for example, Cara et al. 2013).

There have been only a few high quality deep *Chandra* observations of large scale quasar jets allowing detailed studies of evolution along the jet. One example was the jet in PKS 1127-145 (Fig. 2), a radio loud quasar at $z = 1.18$ (Siemiginowska et al. 2007). This jet shows a complex X-ray morphology and substructure within the knots. The X-ray and radio intensity profiles along the jet are quite different, with the radio peaking at the outermost regions of the jets and X-ray emission being strongest in the regions close to the quasar core. "One-zone" emission models fail; at least two components are needed to explain the observations, with the X-rays originating in the proper relativistic jet, and the radio in a surrounding "sheath." The jet in 3C273 shows a similar behavior. Yet some jets, for example PKS 2101-490 (Godfrey et al. 2012a), show the opposite behavior, with the stronger X-rays at the end of a jet. For some other cases, radio and X-ray emission profiles have an almost constant intensity ratio along the jet, typically seen in FR I jets with the X-rays due to the synchrotron emission (Fig. 1). In addition, recent studies of PKS 0637-752 archival data by Godfrey et al. (2012b) revealed a quasi-periodic structure of the jet profile, suggesting a possible modulation in the jet launching process or a presence of re-confinement shocks. Estimates of the jet instantaneous power depend on the true process responsible for these observational trends seen by *Chandra*.

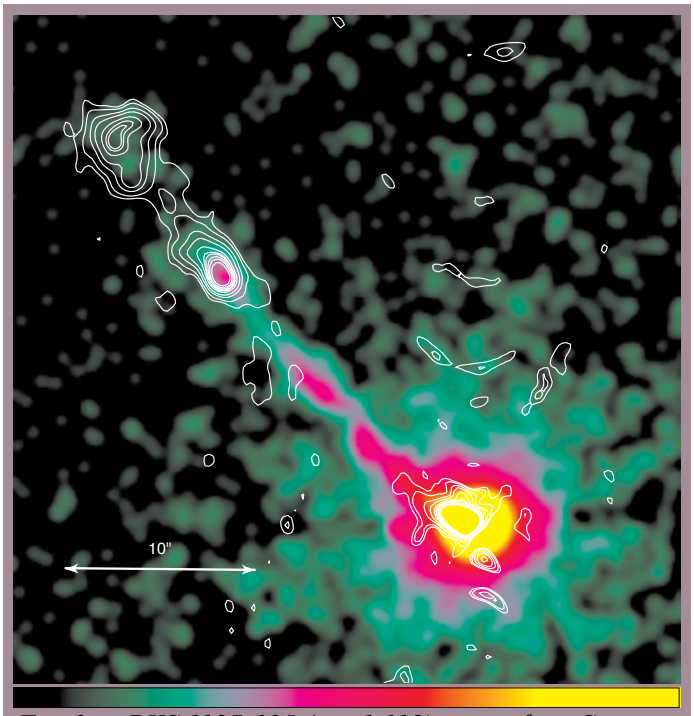

Fig. 2 — PKS 1127-125 (z = 1.118) image from Siemiginowska et al. (2007). The color scale is the smoothed Chandra *ACIS-S image showing a quasar with a jet of the ~ 300 kpc projected length. The contours are from the VLA 8.4 GHz image. The arrows indicate a 10" scale.*

The high quality *Chandra* data indicate the complexity of quasar jets and of the physics responsible for powering jets, and the energy release. These data show that extragalactic jets remain relativistic out to large ~ Mpc distances from their origin, setting timescales for the jet activity stage in the evolving black hole. Important questions related to the physics of

particle acceleration at such large distances from the black hole remain unanswered.

Quasar Jets at High Redshift

Only a handful of high redshift quasar jets has been studied with *Chandra*. The highest redshift X-ray jets to date have been detected in luminous radio quasars, GB 1508+5714 (z = 4.3, Siemiginowska et al. 2003) and GB 1428+4217 (z = 4.72, Cheung et al. 2012). The *Chandra* images are not very impressive, showing only 3″–4″extension on one side of the quasar core with a small number of X-ray counts associated with the radio jets (see Fig. 3). The energy density of the CMB scales as $(1 + z)^4$ and in the simplest IC/CMB scenario, large scale jets with similar Lorentz factors should have the same surface brightness at any redshift (Schwartz 2002). However, this has not been observed; the high-z jets are fainter than these predictions. In fact, assuming the IC/CMB model, the Doppler factor derived for the two $z > 4$ jets of $\delta \sim 3$–6 is lower than observed in low-z jets. This suggests that the high-z jets might be intrinsically less relativistic or they decelerate more rapidly out to ∼ 10s–100s kpc scale than the low-z ones.

The current *Chandra* results for high-z jets are puzzling, but they are based on a just few observations. While most of the X-ray jets studied so far are located at $z < 2$, the highest redshift observations provide the most stringent test of the IC/CMB model. Future *Chandra* observations of a larger sample of kpc-scale radio jets over a broad redshift range at $z > 2$ are necessary. Such data should provide more insights to the jet physics and allow us to study the jets resulting from the "earliest" actively accreting black hole systems.

X-ray Variability of Jets

Jets are expected to vary. The parsec-scale blazar jets unresolved in X-rays show large amplitude flares across the entire electromagnetic spectrum. However, the variations of the larger scale X-ray resolved jet features have only been studied in a few jets with multiple *Chandra* observations.

The best X-ray monitoring data has been collected for the M87 jet, which was observed with *Chandra* more than 60 times between 2002–2008 (Harris et al. 2009) showing the most dramatic flux variability of the HST-1 knot. Initially the X-ray flux of the HST-1 knot increased by a factor of 2 in 116 days in 2002 and the knot faded over several months, but then again in 2005 the X-ray flux increased by a factor of ∼ 50. The 2005 HST-1 flare was monitored by the HST and VLA. These data allowed for multi-frequency studies of the rise and decay times to constrain the emission size and the energy losses of the relativistic electrons. Harris et al. (2009) described details of these studies and concluded that the multi-frequency lightcurves are consistent with E^2 energy losses dominated by synchrotron cooling and yields an average magnetic field strength of 0.6 mG for the knot. Most surprising was the discovery of flux oscillation on a 0.5–0.8 year timescale. The origin of the oscillation remained unidentified, but Harris et al. (2009) suggested that it can be related to quasi-periodic variations in the conversion of the jet kinetic power to the internal energy of the radiating plasma. The HST-1 X-ray flare remains the strongest observed for a knot at a large distance (> 50 pc) from a supermassive black hole. While the X-ray flare of HST-1 happened on timescales longer than a year, the X-ray light-

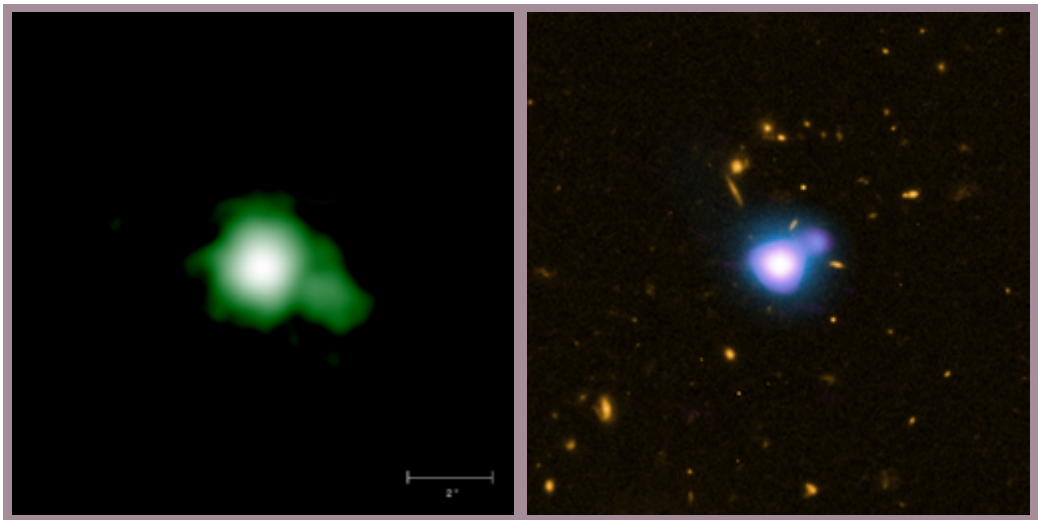

Fig. 3 — The two highest redshift quasar jets detected by Chandra *to date. Left: A smoothed* Chandra *image of the quasar GB 1508+5714 and its jet at* z = *4.3. Right: A combined multiband image of GB 1428+4217 quasar and jet at* z = *4.72 : X-rays are represented as blue, the optical HST as yellow and radio VLA image as purple.*

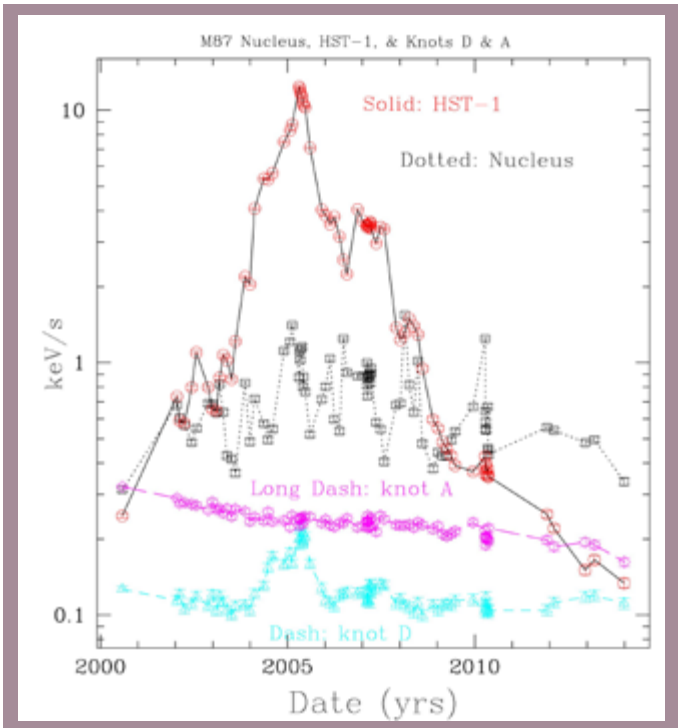

Fig. 4 — X-ray lightcurve of M87 nucleus and three knots HST-1, A, D collected over 13 years of Chandra *monitoring program led by Dan Harris (Harris et al. 2009). A strong and long-lasting outburst of HST-1 knot dominates the lightcurve. The nucleus shows the short-term variability during the same time. During the time HST-1 was peaking, severe pileup corrupted the PSF so that both the nucleus and knot D photometric apertures were collecting a fraction of HST-1 events.*

curve of the nucleus shows a short-term large fractional variability characteristic of the "flickering" suggesting that the TeV flare observed in 2005 may have originated in the nucleus. Monitoring of the M87 jet continues and the future observations should give answers to the critical question about the origin of the large amplitude short-term TeV flare, with important implications for our understanding of the physics associated with the accreting black hole and the relativistic jets.

The galaxy Centaurus A is a factor of ~ 2.5 closer than M87 and *Chandra* data resolved Centaurus A jet into more than 40 knots. Some of these knots have corresponding radio emission, but there are also knots with no radio counterpart. Many observations performed over the timescale of the mission allowed for detailed studies of the individual knots including proper motion, spectra and variability. Goodger et al. (2010) ruled out impulsive particle acceleration as a formation mechanism for the knots and found no evidence for X-ray flux variability. The most likely mechanism for the stationary knots could be a collision resulting in a local shock followed by stable particle acceleration and X-ray synchrotron emission. An apparent motion in three knots was also detected, but there was no conclusive evidence for or against a faster moving "spine" within the jet.

The X-ray variability of high power large scale jets associated with quasars and FRII radio galaxies has not been studied in a systematic way. The knots in these powerful jets are larger and less resolved than in the two nearby FRI radio galaxies that have been monitored. Larger knots mean longer characteristic timescales. Only a small number of quasar jets have been observed more than once with *Chandra* during the last 15 years. The famous 3C273 quasar jet has several observations in the archives, but the variability analysis by Jester et al. (2006) did not show any significant changes in the X-ray knots. The only reported variability of the X-ray knot located at a large distance from the nucleus was in Pictor A (Marshall et

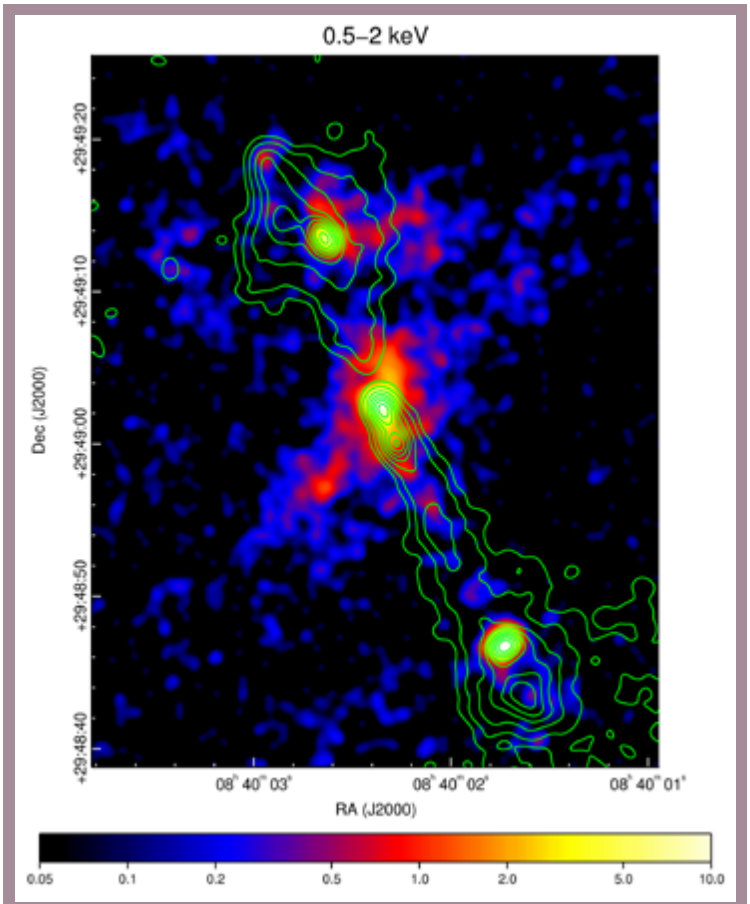

Fig. 5 — 4C+29.30 X-ray image with radio contours from Siemiginowska et al. (2012). Compare to the multiband composite image on the cover of this Newsletter.

al. 2010), where the X-ray knot disappeared between the *Chandra* observations of 2000 and 2002. Pictor A is a FRII radio galaxy with the projected jet length of about 150 kpc. An X-ray flare of the knot located ~ 35″ from the core is a surprise. Given the timescales of the synchrotron losses, the size of the flaring region must be significantly smaller than the knot and characterized by a much larger magnetic field than the average over the entire jet. *Chandra* follow-up observations of Pictor A should provide some more insight to the behavior of this knot.

Jet Impact on the ISM

The cover of this Newsletter issue displays a multi-band image showing complex morphology resulting from the jet outflow in a nearby elliptical galaxy 4C+29.30 ($z = 0.0649$). 4C+29.30 could be viewed as an analog to the famous radio galaxy Centaurus A, but more distant and more powerful in the radio. It displays a similar morphology with a pronounced dust lane and cold gas stretching across the galaxy, perpendicular to the radio source axis. The 4C+29.30 radio source extends ~ 30 kpc from the center of the galaxy, showing a prominent one-sided jet but with lobes both south and north. The galaxy contains a strong extended optical emission-line region at a similar distance from the center located at the edge of the elliptical galaxy. The *Chandra* deep image shows complex X-ray emission spanning about ~ 60 kpc in total extent, marked by a pronounced center and two bright components coincident with the jet termination regions (the radio "hotspots," See Fig. 5). Faint diffuse X-ray emission traces the jet and connects the two hotspots, but extends beyond the radio emitting regions and shows several filaments. The bright X-rays north of the nucleus overlap with the clouds of line-emitting gas. There is also diffuse emission perpendicular to the jet axis across the center. so that the X-ray image gives an overall impression of an X-shaped structure.

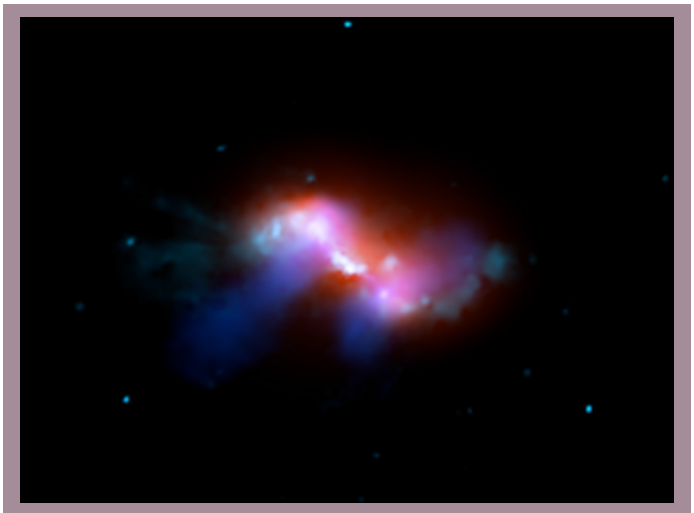

Fig. 6 — The interacting jet of the radio galaxy 3C305 (z = 0.0416). A composite multiband image shows smoothed Chandra *X-rays in orange, radio in blue, and optical in green (Hardcastle et al. 2012).*

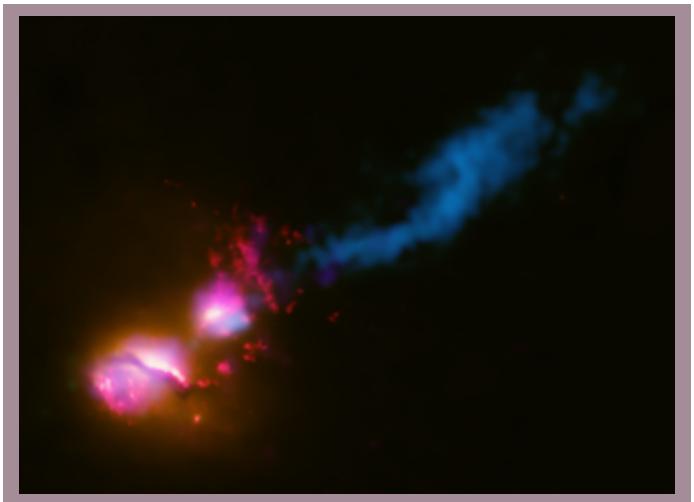

Fig. 7 — The interacting jet of the radio galaxy 3C321. A composite multiband image shows X-ray data from Chandra *(purple), optical and ultraviolet (UV) data from HST (red and orange), and radio from the VLA and MERLIN (blue). A bright, blue spot in the VLA and MERLIN radio image shows where the jet has struck the side of the galaxy and dissipates some energy. The jet is disrupted and deflected by this impact with the companion galaxy (Evans et al. 2008).*

The *Chandra* observation of 4C+29.30 contributes to studies of the physics of radio source interactions with the ISM. This deep X-ray image allowed us to assess the overall energetics of the system with detail much-improved over the earlier studies in the radio and optical bands. The spectral analysis carried out for several of the brightest X-ray features indicated a mixture of thermal and non-thermal emission components, characterized by a variety of temperatures and spectral slopes. Possible variations in metal abundances of the hot ISM were also detected with high abundances in the center and the very low values (< 0.1 of the Solar) in the outer regions of the galaxy. The X-ray emission of the jet and the hotspots seems to be particularly complex, with different and distinct emission components, both thermal and non-thermal (synchrotron and/or inverse-Compton). The synchrotron model for the X-ray jet is favored, but there are

large uncertainties and higher quality data are required for a statistically significant result.

It is in any case evident that a significant fraction of the jet energy (jet power, $L_j \sim 10^{42}$ erg s^{-1}) goes into heating the surrounding gas and the X-ray data support the heating of the ambient medium via weak shocks (Mach number M = 1.6). Only a small amount of the jet power is needed to accelerate clouds of colder material that are dragged along the outflow. The nucleus of the galaxy is surprisingly powerful in X-rays ($\sim 10^{44}$ erg s^{-1}) and heavily obscured by a significant amount of matter ($N_H \sim 5 \times 10^{23}$ cm^{-2}) falling towards the center (also indicated by HI absorption lines) (Sobolewska et al. 2012). This infall may be related to the feeding of the nucleus and triggering the current jet activity. The nucleus is sufficiently luminous to photo-ionize the whole extended emission-line region. These results support and strengthen conclusions regarding the feedback process operating in 4C+29.30 (Siemiginowska et al. 2012).

The direct impact of the jet on the interstellar medium in galaxies is evident. Details of jet-ISM interactions can be traced in several deep *Chandra* observations including M87 (Million et al. 2010), Cen A (Hardcastle et al. 2007) and a nearby Seyfert 1 galaxy NGC 4151 (Wang et al. 2011). Many observations indicate the presence of jet-induced outflow associated with optically emitting clouds. The signatures of a jet-induced shock with relatively low Mach number capable of heating the gas are also found in a few galaxies (see for example Fig. 6 and 7), providing strong evidence for the jet impact on the ISM and the importance of jets for the evolution of galaxies.

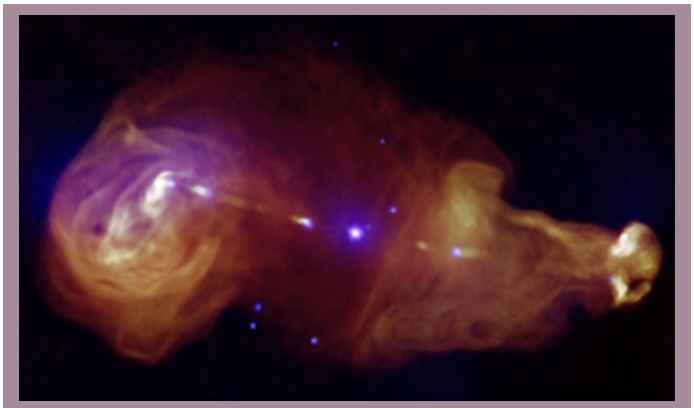

Fig. 8 — A composite image of 3C353 (z = 0.0304), an FR II radio galaxy: radio VLA (yellow) and Chandra *X-rays (blue). Two broad jets, hotspots and lobes are visible in the radio band. X-ray emission is detected in most radio structures: the nucleus, the jet and the counterjet, the terminal jet regions (hotspots), and one radio lobe. The X-rays associated with the knots and counterknots are inconsistent with the IC/CMB emission models (Kataoka et al. 2008).*

Summary and Future Perspectives

Chandra has initiated the X-ray studies of extragalactic jets. The first 15 years of *Chandra* observations indicate that jet X-ray emission is universal and that most jets can be detected in high spatial resolution X-ray observations of sufficient depth. The jet physics highlighted by the *Chandra* studies is complex, but the current high quality data have already provided important constraints on the emission process and on particle acceleration in radio galaxies. There are, however, many outstanding questions born from the *Chandra* observations and related to the energetics, particle acceleration and emission processes in powerful quasar jets. A few deep studies show that the jet morphology is complex, with fast and slow moving regions, and compact knots embedded in the more uniform diffuse emission. Signatures of complex interaction with the environment are seen in many observations of nearby jets, giving some early constraints on jet lifetime and evolution. More *Chandra* observations of jets are necessary to provide good statistical samples for studies of jets in general. The archival legacy of *Chandra* continues to be one of the most important goals in this field. With no new high angular resolution X-ray mission planned for the near future, *Chandra* remains our only choice for the X-ray studies of jets.

The author thanks Dan Harris for a careful reading of this letter and insightful comments.

References

Baade, W., & Minkowski, R. 1954, ApJ, 119, 215

Cara, M., et al., 2013, ApJ, 773, 186

Celotti, A., Ghisellini, G., & Chiaberge, M., 2001, MNRAS, 321, L1

Cheung, C. C., Stawarz, Ł., Siemiginowska, A., et al. 2012, ApJ, 756, L20

Evans, D. A., Fong, W. F., Hardcastle, M. J., et al. 2008, ApJ, 675, 1057.

Feigelson, E. D. 1980, Ph.D. Thesis

Godfrey, L. E. H., Bicknell, G. V., Lovell, J. E. J., et al. 2012, ApJ, 755, 174

Godfrey, L. E. H., Lovell, J. E. J., Burke-Spolaor, S., et al. 2012, ApJ, 758, L27

Goodger, J. L., Hardcastle, M. J., Croston, J. H., et al. 2010, ApJ, 708, 675

Hardcastle, M. J. 2006, MNRAS, 366, 1465

Hardcastle, M. J., Kraft, R. P., Sivakoff, G. R., et al. 2007, ApJ, 670, L81
Hardcastle, M. J., Massaro, F., Harris, D. E., et al. 2012, MNRAS, 424, 1774
Harris, D. E., & Krawczynski, H. 2006, ARA&A, 44, 463
Harris, D. E., Cheung, C. C., Stawarz, Ł., Biretta, J. A., & Perlman, E. S. 2009, ApJ, 699, 305
Harwood, J. J., & Hardcastle, M. J. 2012, MNRAS, 423, 1368
Hogan, B. S., Lister, M. L., Kharb, P., Marshall, H. L., & Cooper, N. J. 2011, ApJ, 730, 92
Jester, S., Harris, D. E., Marshall, H. L., & Meisenheimer, K. 2006, ApJ, 648, 900
Kataoka, J., Stawarz, Ł., Harris, D. E., et al. 2008, ApJ, 685, 839
Marshall, H. L., Miller, B. P., Davis, D. S., et al. 2002, ApJ, 564, 683
Marshall, H. L., Hardcastle, M. J., Birkinshaw, M., et al. 2010, ApJ, 714, L213
Marshall, H. L., Gelbord, J. M., Schwartz, D. A., et al. 2011, ApJS, 193, 15
Massaro, F., Harris, D. E., & Cheung, C. C. 2011, ApJS, 197, 24
Million, E. T., Werner, N., Simionescu, A., et al. 2010, MNRAS, 407, 2046
Mingo, B., Hardcastle, M. J., Croston, J. H., et al. 2011, ApJ, 731, 21
Perlman, E. S., Biretta, J. A., Sparks, W. B., Macchetto, F. D., & Leahy, J. P. 2001, ApJ, 551, 206
Pudritz, R. E., Hardcastle, M. J., & Gabuzda, D. C. 2012, Space Sci. Rev., 169, 27
Sambruna, R. M., Gambill, J. K., Maraschi, L., et al. 2004, ApJ, 608, 698
Schreier, E. J., Feigelson, E., Delvaille, J., et al. 1979, ApJ, 234, L39
Schreier, E. J., Gorenstein, P., & Feigelson, E. D. 1982, ApJ, 261, 42
Schwartz, D. A., Marshall, H. L., Lovell, J. E. J., et al. 2000, ApJ, 540, L69
Schwartz, D. A. 2002, ApJ, 569, L23
Siemiginowska, A., Smith, R. K., Aldcroft, T. L., et al. 2003, ApJ, 598, L15
Siemiginowska, A., Stawarz, Ł., Cheung, C. C., et al. 2007, ApJ, 657, 145
Siemiginowska, A., Stawarz, Ł., Cheung, C. C., et al. 2012, ApJ, 750, 124
Sobolewska, M. A., Siemiginowska, A., Migliori, G., et al. 2012, ApJ, 758, 90
Tavecchio, F., Maraschi, L., Sambruna, R. M., & Urry, C. M., 2000, ApJL, 544, L23
Willingale, R. 1981, MNRAS, 194, 359
Wang, J., Fabbiano, G., Elvis, M., et al. 2011, ApJ, 736, 62
Worrall, D. M. 2009, A&A Rev., 17, 1